Inorganic Chemistry

pubs.acs.org/IC

Article

Open Access

This article is licensed under CC-BY 4.0

10-Valence-Electron C≡O and the 14-VE C≡Pt: Two Triple-Bonded Isoelectronic Families Differing by a $d\delta^4$ Ring

Michiko Atsumi* and Pekka Pyykkö*

Cite This: *Inorg. Chem.* 2023, 62, 21083−21090

Read Online

ACCESS | Metrics & More | Article Recommendations

ABSTRACT: 10-VE A≡A′ Diatomics, such as N≡N, C≡O, etc., have a strong $\sigma^2\pi^4$ triple bond plus a lone pair at each end. In our studies on 14-VE A≡B systems, such as C≡Pt, we find a similar bonding system plus a $(5d\delta)^4$ ring. Here, the A atom belongs to groups 13−17 and the B atom to groups 7−11. Also the BB′ combinations, triatomics, such as PtCO or DsCO or uranyl, and longer chains, such as AuCN and [NC-Au-CN]$^-$, are discussed. The δ ring directly contributes to nuclear quadrupole coupling constants, and DFT calculations using the BH and H or mPW1K functionals reproduce the experimental trends of the NQCC.

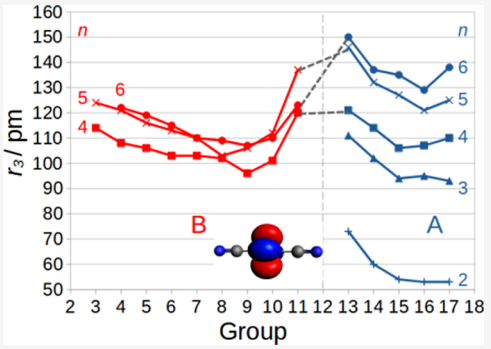

Downloaded via 46.9.61.21 on February 18, 2024 at 21:45:10 (UTC).
See https://pubs.acs.org/sharingguidelines for options on how to legitimately share published articles.

1. INTRODUCTION

While developing a set of additive covalent triple-bond radii, r_3,[1,2] the same covalent radii $r(A)$ were used in fitting the main-group A≡A′ and the A≡B bond lengths, where B is a transition metal. The primary bond lengths came from experimental or computed closed-shell systems with main-group elements and with transition metals as long as the molecular-orbital inspection and the actual bond length fitted the picture. The same covalent radii $r(A)$ were used in fitting the main-group A≡A′ and the A≡B bond lengths for both single, double, and triple bonds, r_1, r_2, and r_3, respectively.

In our ongoing calculations, we kept finding two different sets of diatomic species. One was the well-known 10VE family of diatomic systems, such as N_2, CO, CN^-, NO^+, etc. These are known to have a nominal $\sigma^2\pi^4$ triple bond combined with a lone electron pair at each end. In all, we then have 10 valence electrons (10VE)[3] (it should be noticed that, as an alternative to this triple-bond picture, in older literature, a C=O double bond was thought to exist, and also other resonance hybrids have been mentioned, see Pauling[4] or Long and Walsh[5]).

The other families, such as CPt, $X^1\Sigma$ had four more electrons, always occupying a δ^4 ring, typically the penultimate, HOMO − 1. With this, we mean the occupied $(d_{xy})^2(d_{x^2-y^2})^2$ combination, in an alternative form $d(l=2,m_l=\pm 2)^4$, or $(d\delta)^4$. The novelty is that we have an occupied orbital which is formally a nonbonding core orbital but has the size and orbital energy of a typical valence orbital. That observation is not new, and some previous examples are shown in Table 1. We are, however, not aware of any previous articles concentrating on this feature.

Starting from these 10-VE or 14-VE families of species, we made some further contacts:

Table 1. Examples on δ^4 Systems

year	species	ref
1998	CAu^+	Barysz,[8] Pyykkö[9]
1999	NIr	Ram[10]
2003	SiPt	Barysz[11]
2004	CPt	Patzschke[12]
2015	SiNi	Schoendorff[13]
1985	$[XAuX]^-$	Bowmaker[14]
1985	$[NC\text{-}Au\text{-}CN]^-$	Bowmaker[14]

1 It also is possible to have the δ^4 ring without any triple bonds to the metal.

2 In multiple bonds between two B atoms, bond orders beyond 3 can be reached, see Cotton et al.[6]

3 One way to "see" the δ^4 electrons is to measure nuclear quadrupole coupling constants. While many DFT functionals have problems in reproducing the electric field gradient (EFG), q, at transition-metals,[7] we have now found two functionals that work. We also report some results for species, not involving the δ^4.

Received: August 18, 2023
Revised: October 27, 2023
Accepted: October 31, 2023
Published: December 5, 2023

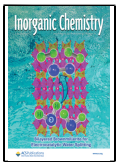

© 2023 The Authors. Published by American Chemical Society

2. METHODS

We use in the present calculations DFT and ZORA at either the scalar relativistic (SR) or spin−orbit (SO) level. This will provide reasonable accuracy and easy interpretation of chemical bonding questions.

The calculations were carried out by using the ADF software package[15] with the Perdew−Burke−Ernzerhof (PBE) functional during the structural calculations. The triple-ζ basis sets with two polarization functions (TZ2P) were used for all elements, treated at the nonfrozen core level.

We have added into Tables 2, 3, 4, 5, and 6 the results of some earlier calculations and a comparison with the sum[a] of our triple-bond covalent radii r_3.[1,2]

3. RESULTS

3.1. Diatomics. Table 2 gives the bond lengths of the A≡B diatomics, specified in Figure 1, mostly for 14VE species.

Table 2. Calculated and Experimental Bond Lengths, R_e, for AB Diatomics[a]

	R_e/pm				
AB	PW	exp	calc	r_3	δ
BRh[d]	170.36[b]	169.2	168.5[16]	179	H
BPt^-	181[b]		179.90[1]	183	H-1
	180.9[c]				
BAu	192.1[b]		192.27[1]	196	H-2
	191.6[c]		190.6[17]		H-1
CNi	160.5[b]	162.73[18]	159.60[1]	161	H-1
CRu[d]	160.9[b]	160.5485(2)[19]	160.1[19]	163	H
			160.42[20]		
CPd	172.2[b]	172.2	171.6[1]	172	H-1
	172.3[c]				
CPt	168.3[c]	167.7[21]	172.5[12]	170	H-1
	167.8[b]		167.45[1]		H-1
CAu^+	178.9[b]		176.6[8,9]	183	H-2
	178.8[c]				
CDs	172.2[b]		172.7[12]	172	
	172.6[c]				
NIr	160.8[c]	160.68281(35)[10]	160.9[10]	161	H-1
SiNi	201.2[b]	203.165(24)[22]	208.6[13]	203	H
SiPt	208.2[b]	206.29(2)	210[11]	212	H-1
	208.7[c]				
$SiAu^+$	219.3[b]		218.8[8]	225	H-2
	219.4[c]				
PIr	198.3[b]	199.28[e,23]		201	H
	199.9[c]				
TlAu	269[b]			273	H-1
	266.6[c]				
BiP	229.5[b]	229.61520(80)[24]		229	
	230.2[c]				
BiAu	258.6[b]			258	H-1
	263[c]			258	H-2,H-3

[a]δ gives the energetic placement of the $d\delta^4$ MO with respect to the HOMO (H). "PW": Present work. r_3: From triple-bond covalent radii.[1,2] [b]SR. [c]SO. [d]12VE species. [e]R_0.

These AB R_e values in Table 2 are close to the sum of triple-bond covalent radii. To the contrary, the BB′ ones in Table 3 can be much shorter, reflecting a bond order higher than three. Quadruple bonding in ground or excited states of certain AB diatomics[20,25] and BB systems[6] has also been discussed.

Liu et al.[26] consider the donation and its direction in certain multiply bonded AA′ diatomics. Cheung et al.[16] also discuss 4-fold bonding in RhB. The MU species (M = Cr−W) of Ruipérez et al.[27] have the δ ring as the HOMO, see Table 3. Note that at the scalar relativistic level, these are 12-VE species with a $(1\pi)^4(1\sigma)^2(2\sigma)^2(1\delta)^4\ X^1\Sigma$ ground state, see ref 27 Figure 1.

Table 3. Calculated and Experimental Bond Lengths, R_e for BB′ Diatomics[a]

	R_e/pm				
BB′	PW	exp	calc	r_3	δ
Cr_2	159.5[b]	167.88	156.2[28]	206	H
CrU	185.4[b]		188.3[27]	221	H
	187.6[c]				
MoU	202.8[b]		202.1[27]	231	H
	205.9[c]				
WU	208.5[b]		208.0[27]	233	H
	217.5[c]				
ThU	248.2[b]			254	H
	279.3[c]				H
ThPt	237.3[b]	254[29]	250[11]	246	H
	237.7[c]				
$ThAu^+$	271.6[b]		263[1]	259	H-1
	262.4[c]				

[a]δ gives the energetic placement of the $d\delta^4$ MO with respect to the HOMO (H). PW: Present work. r_3: From triple-bond covalent radii. [b]SR. [c]SO.

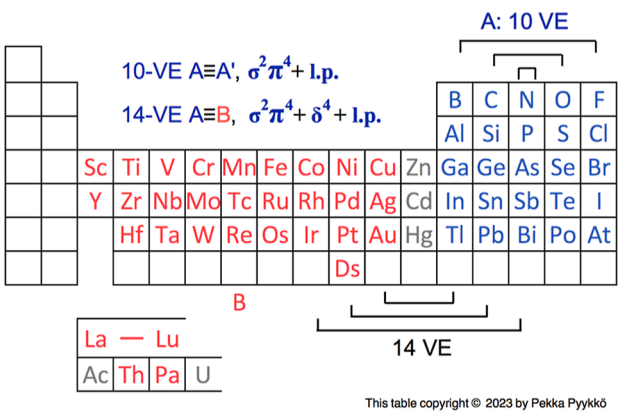

Figure 1. Schematic placement of the main-group elements (A) and transition elements (B). The 10VE A≡A′ and 14VE A≡B combinations are indicated. l.p. = lone pairs.

3.2. Polyatomic Chains. If group 11 (Cu, Ag, Au, and Rg) doubles as a halogen and group 10 (Ni, Pd, Pt, and Ds) as a chalcogen, it is easy to take the step from OCO to PtCO or DsCO.[12] With metals at both ends, we have $[Au{=}C{=}Au]^{2+}$, or the analogues CPt, CPt_2, and CPt_3^{2-} to CO, CO_2, and CO_3^{2-}, respectively.[30]

Of the species in Table 4, the triatomic PtCPt and $[AuCAu]^{2+}$ have two δ^4 rings, both a *g* and a *u* one, separated from each other by the carbon atom.

Similarly, the uranyl isoelectronic series[31] would yield NUN and the NUIr of Gagliardi and Pyykkö.[32] The NUO^+ predicted by Pyykkö et al.[31] was later made by Heinemann and Schwarz[33] in the gas phase and by Zhou and Andrews[34] in Ne matrices. The $OUIr^+$ was prepared by Santos et al.[35] For reviews on uranyl analog complexes, see Wei et al.,[36] or Maria and Marçalo.[37] A closer analysis of U≡A multiple bonding was given by Motta and Autschbach.[38]

With 5d metals at both ends, linear species like $PtThIr^-$ were found by Hrobárik et al.[39] This species had a δ^4 ring at the Pt

https://doi.org/10.1021/acs.inorgchem.3c02889
Inorg. Chem. 2023, 62, 21083−21090

Table 4. Calculated and Experimental Bond Lengths, R_e, for Linear Polyatomic Species[a]

		R_e/pm				
species	bond	PW	exp	calc	r_3	δ
AuCN[c]	Au−C	190.6	191.51[45]		183	H-2
	C−N	116.9	115.56[45]		114	
$[NCAuCN]^{-1}$[b]	Au−C	198.8	198.4[d]	198.8[43]	183	H-2
				199[46]		
$[HAuCN]^{-1}$	Au−C	207.4[b]		202.5[47]	183	H-2
		202.1[c]				
$[FAuF]^{-}$	Au−F	199.9[b]		196.3[43]	176	H-2
		199.3[c]				
$[ClAuCl]^{-}$	Au−Cl	230.2[b]	228	228.3[43]	216	H-2
		229.6[c]		228.3[48]		
$[BrAuBr]^{-}$	Au−Br	242.2[b]	240	239.4[43]	233	H-2
		241.5[c]		240.8[48]		
$[IAuI]^{-}$	Au−I	259.6[b]	253	256.1[43]	248	H-2
		259.2[c]		256.9[48]		
$[AtAuAt]^{-}$	Au−At	268.6[b]		263.9[43]	261	H-3
		270.2[c]				
PtCO	Pt−C	176.1[b]	176.046[49]	177.6[30]	170	H
PtCPt	Pt−C	173.8[c]		173.5[30]	170	H-2
$[AuCAu]^{2+}$	Au−C	182.6[b]		173.5[30]	183	H-2
		182.4[c]				
NUIr	N−U	173.9[b]		172.2[32]	172	H-1
		179.8[c]				
	U−Ir	217[b]		218.4[32]	225	H-1
		222.5[c]				
$OUPt^{2+}$	O−U	172.7[b]		171.4[50]	171	H-1
		174.3[c]				
	U−Pt	228.6[b]		221.4[50]	228	
		229[c]				

[a]The $[XAuX]^{-}$ experimental values for X = Cl−I are taken from.[44] In the last column, the δ gives the energetic placement of the $d\delta^4$ MO with respect to the HOMO (H). Slight variations of the order may occur as a function of the method. PW: Present work. r_3: From triple-bond covalent radii. "Calc." refers to earlier calculations. [b]SR. [c]SO. [d]In $Nd[Au(CN)_2]_3{\cdot}3H_2O$.[51]

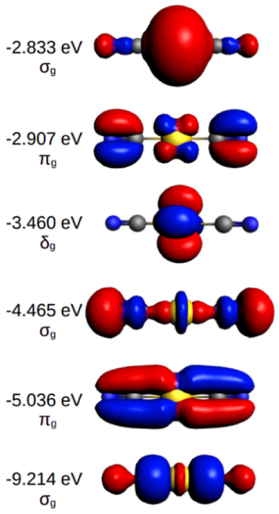

Figure 2. Highest occupied MO/s of a free $[NC\text{-}Au\text{-}CN]^{-}$ anion. The δ^4 ring is the HOMO − 2 one at −3.460 eV.

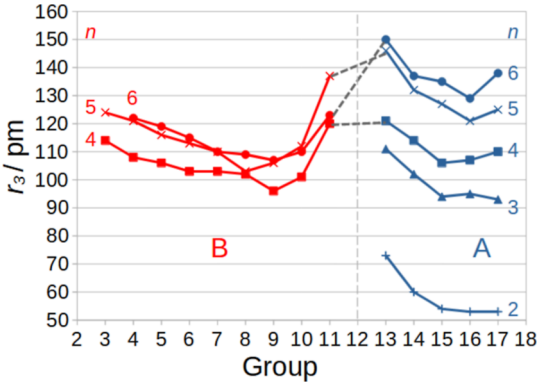

Figure 3. Additive triple-bond covalent radii, r_3 (in pm), for transition-metal atoms (B) and main-group elements, (A) belonging to the groups 3−11 and 13−17, respectively. n is the number of the row.

end, and some evidence for Th−Ir δ bonding at the Ir end. Two of the σ bonds were characterized as "a sausage inside a tube".

The isoelectronic series of $[ClAuCl]^{-}$ can be continued at least to the high-pressure compound Li_5AuP_2.[40] The energetic location of the δ^4 ring in the $[XAuX]^{-}$ series, X = F−At, is discussed in the last column of Table 4.

Pauling[41] considered a δ bond in $Re_2Cl_8^{2-}$, an assigned quadruple-bond case. For further examples, see the book.[6] He also found two triple U≡O bonds in uranyl. Possible members of the uranyl isoelectronic series down to $[CUC]^{2-}$ have been discussed.[31]

Most of the World's gold production[42] is based on the $[NC\text{-}Au\text{-}CN]^{-}$ ion, which has a beautiful δ ring, as seen from Figure 2. This δ energy level occurred as H-2 also in earlier calculations.[43]

https://doi.org/10.1021/acs.inorgchem.3c02889
Inorg. Chem. 2023, 62, 21083−21090

Table 5. Vibrational Frequencies, ω_e (cm^{-1}), for Diatomics

	ω_e/pm		
species	PW	exp	calc
BRh[c]	939[b]		
BPt^-	844[a]		
	842[b]		
BAu	658[a]		
		704[17,d]	710[17]
BAu	663[b]		
CNi	959	875.155[18]	
CRu[c]	1156[b]	1100[19]	
CPd	885[a]		
	881[b]		
CPt	1059[b]	1051.13(2)[21]	1096[12]
CAu^+	827[a]		873[8]
	826[b]		
CDs	1115[b]		1147[12]
NIr	1166[b]	1126.1757(28)[10]	1161[10]
		1195(38)[54,e]	
SiNi	499[a]	467.43[22]	458[13]
	497[b]		
SiPt	537[a]	549.0(3)	531[11]
	527[b]		
$SiAu^+$	427.2[a]		459[8]
	426.6[b]		
PIr	624[a]	570[23]	
	591[b]		
TlAu	135[a]		
	139[b]		
BiAu	168[a]	157.7[55]	
ThPt	248[a]	221[29]	211[11]
	245[b]		
$ThAu^+$	143[a]		188[11]

[a]SR. [b]SO. [c]12VE species. [d]r_0. [e]In noble-gas matrices.

Table 6. Vibrational Frequencies for Polyatomic Species[b,c]

		ω_e/cm^{-1}		
species	mode	PW	exp	calc
AuCN	$\nu_1(\sigma)$	2161		2276,[45] 2181[56]
	$\nu_2(\pi)$	335	320[45]	313″, 285[56]
	$\nu_3(\sigma)$	474	480[45]	476″, 472[56]
$[Au(CN)_2^-]$	C−Nσ_u	2130	2158[a,51]	
	C−N σ_g	2147	2166[51]	
	Au−C σ_u	403	474, 491[51]	
	Au−C π_u	420		
	Au−C σ_g	427		
	π_g	290		
	π_u	80		
$AuCl_2^-$	σ_g	300.6	329[57]	310[43]
	σ_u	320.9	350[57]	330″
	π_u	110.5	116[57]	103″
$AuBr_2^-$	σ_g	193	209[57]	194″
	σ_u	238	254[57]	238″
	π_u	74.6	77[57]	69″
AuI_2^-	σ_g	142	158[57]	143″
	σ_u	200	210[57]	194″
	π_u	55.8	63[57]	52″

[a]In solid $Nd[Au(CN)_2]_3{\cdot}3H_2O$. [b]SR. [c]12VE species.

3.3. Other Properties. *3.3.1. Relation of Bond Lengths and the Triple-Bond Covalent Radii.* Both A≡A′ and A≡B triple bonds with various principal quantum numbers, n, were used to originally fit the additive r_3. As seen from Tables 2 and 3, the present R mostly agree with

$$R(AB) = r_3(A) + r_3(B) \quad (1)$$

for triple bonds. The higher bond-orders in Table 3 may be substantially shorter.

Clear trends as a function of the group and the row are seen in Figure 3. For the shortness of the $n = 2$ radii, see Wang et al.[52] Note for the n-dependence of the main-group elements A the clear trend $2 \ll 3 < 4 < 5 < 6$, while the transition metals, B, in the groups 9−10 rather have $6 < 5 \approx 4$. The sixth-row elements near gold have a local maximum of the relativistic bond-length contraction.[53]

Vibrational frequencies are another direct connection to experiments. As examples, we can take Table 5 on diatomics or Table 6 on polyatomic chains.

Dissociation energies and predissociation of species like CuB, AuB, or AlB are discussed by Merriles and Morse.[58] The δ MO is quoted in their Supporting Information.

Nuclear quadrupole coupling constants, NQCCs, give a direct access to the electric field gradient, q at the nuclei involved. The four electrons in the δ^4 ring make a major contribution. The RuC has been mentioned as an example by Wang et al.,[19] who estimate that +1350 MHz of the experimental B_0 of +433 MHz of ^{101}RuC come from the δ^4 ring. Without this contribution, even the sign would be wrong. Gusmão et al.[59] obtained similar q values for RuC.[b]

For nuclear quadrupole coupling constants, BHandH and mPW1K functionals were applied. The BHandH gave earlier good q for HCl and CuCl,[60] $CdMe_2$,[61] and $Cd(SMe)_2$.[62]

In early multiple-scattering Xα calculations, Bowmaker et al.[14] gave an orbital-based analysis of their q and found for $[Au(CN)_2^-]$ that about +15.805 of the total q of −9.650 au arise from the H-4 δ^4 electrons. They emphasized in their scalar-relativistic discussion of the AuX_2^- species the q contributions from the Au $6p_z$ orbital.

In the linear $HAuH^-$ both the Au 5dπ and 5dδ would be "inert" and only the Au 6s and 5dσ participate in bonding, as seen from Figure 4. The AuH_2^- anion has been seen in matrix spectroscopy[63] and photoelectron spectroscopy.[64]

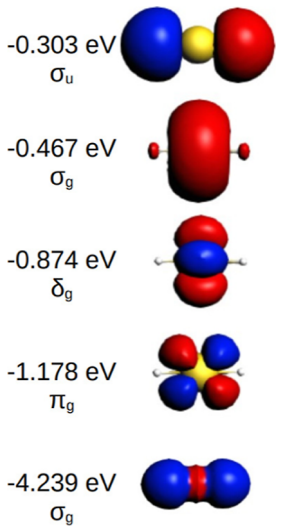

Figure 4. Highest occupied orbitals of the AuH_2^- anion. The result resembles Figure 6 of Liu et al.[64]

https://doi.org/10.1021/acs.inorgchem.3c02889
Inorg. Chem. 2023, 62, 21083−21090

Table 7. Calculated (SO) and Experimental NQCC, $B_e = e^2qQ/h$ (MHz), at the SO Level, Assuming the Q Values in Table 8

		B_e/MHz		
species	Nucl	PW	exp	calc
BRh	^{11}B	−1.29[b]		
BPt$^-$	^{11}B	−3.47		
BAu	^{11}B	−4.41		
	^{197}Au	260.0		
CNi	^{61}Ni	89.2		
CRu[c]	^{101}Ru	544.7	433.19(8)[19]	476.24[c,19]
CPd	^{105}Pd	370.5		
CAu$^+$[a]	^{197}Au	322.9		
NIr	^{14}N	−4.69		
	^{103}Ir	1951.7	1721[c,71]	
SiNi	^{61}Ni	78.0		
SiAu$^+$	^{197}Au	219.5		
PIr	^{103}Ir	1484.2	1424[c,71]	
BiN	^{209}Bi	1101.3	905.066(88)[24]	
	^{14}N	−2.91	−2.468(13)[24]	
BiP	^{209}Bi	1110.0	903.031[24]	
TlAu	^{197}Au	93.5		
BiAu	^{209}Bi	−237.4		
	^{197}Au	151.3		
ThPt	^{229}Th	−3759.1		
CrU	^{53}Cr	−1.59		
	^{235}U	1547.3		
MoU	^{95}Mo	6.87		
	^{235}U	291.4		
WU	^{235}U	6823.2		
AuH	^{197}Au	164.3	187.116(99)[72]	
AuD	^{197}Au	164.3	188.119(33)[72]	
AuF	^{197}Au	−72.6	−52.2344(67)[73]	
AuCl	^{197}Au	2.61	9.63312(13)[74]	
	^{35}Cl	−60.1	−61.99694(81)[74]	
AuBr	^{197}Au	25.9	37.2669(14)[74]	
	^{79}Br	463.8	492.3271(12)[74]	
AuI	^{197}Au	58.5	78.273(11)[75]	
	^{127}I	−1703.9	−1707.881(25)[75]	

[a]Assumed Q/mb from Pyykkö,[76] unless otherwise stated: ^{11}B 40.59(10), ^{14}N 20.44(3), ^{53}Cr 150(50), ^{61}Ni 162 mb, ^{101}Ru 457(23), ^{100}Rh 153, ^{105}Pd 660(11), ^{193}Ir 751(9), ^{197}Au 547(16). ^{209}Bi 422(3)[77] and references there. ^{229}Th 3110(60), ^{235}U 4936(6). [b]12VE species. [c]At $v = 0$.

Table 8. Calculated (SO) and Experimental NQCC, $B_e = e^2qQ/h$ (MHz), at the SO Level for Polyatomic Species, Assuming the Q Values[a]

		B_e/MHz		
species	Nucl	PW	exp	calc
AuCN	^{197}Au	−23.2	−0.7246(46)[65]	
	^{14}N	−5.01	−4.1522(17)[65]	
$AuCl_2^-$	^{197}Au	−648.3	(−)765[b], (−)802	−862.5[14]
				−721[14]
			(−)785[76]	
	^{35}Cl	−35.6	(−)35.2[14,79]	
$AuBr_2^-$	^{197}Au	−620.3	(−)790(50), (−)794[78]	−692[14]
	^{79}Br	248.9		202[14]
AuI_2^-	^{197}Au	−590.4	(−)718, (−)719[78]	−709[14]
$Au(CN)_2^-$	^{197}Au	−1325.9	(−)1263	−1118[14]
			(−)1206[78]	
$AuAt_2^-$	^{197}Au	−488.2		
AuD_2^-	^{197}Au	−1347.3		
HAuCN$^-$	^{197}Au	−1348		
	^{14}N	−4.80		
NUIr	^{14}N	−1.30		
	^{235}U	−4308.6		
	^{193}Ir	1139.1		
OUPt^{2+}	^{17}O	0.84		
	^{235}U	−1199.1		

[a]Assumed Q/mb from Pyykkö,[78] unless otherwise stated: ^{11}B 40.59(10), ^{14}N 20.44(3), ^{53}Cr 150(50), ^{61}Ni 162 mb, ^{101}Ru 457(23), ^{100}Rh 153, ^{105}Pd 660, ^{193}Ir 751(9), ^{197}Au 547(16). ^{209}Bi 422(3)[77] and references there. ^{229}Th 3110(60), ^{235}U 4936(6). The Au NQR frequencies of Bowmaker[14] have been scaled by a Q-ratio of (547 mb/590 mb) = 0.927. [b]See[80].

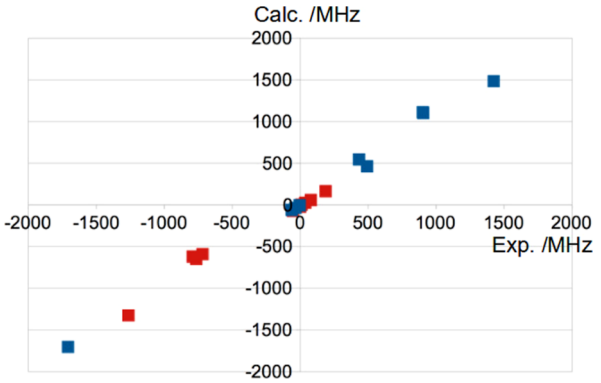

Figure 5. Comparison between calculated (PW) and experimental B. The data are taken from Tables 7 and 8. The red dots refer to B(Au) and the blue dots refer to other nuclei.

In actual fact, one must emphasize that the XAuX$^-$ calculations show some unusually strong dependence on the chosen functional.[57] Moreover, the Mössbauer measurements are performed on solid samples with so far unknown matrix effects.

The gas-phase measurements included in Tables 7 and 8 have a chance to provide cleaner comparisons. The gas-phase microwave quadrupole coupling constants of Okabayashi et al.[65] for triatomic AuCN were in complete disagreement with our earlier calculations, while their structural and vibrational AuCN parameters are in adequate agreement both with our more approximate work, and the latest and best studies.[56,66] Then, we found that the alternative functionals BHandH and mPW1K gave a semiquantitative agreement between the experimental and calculated B, as seen from Figure 5.

As one point of reference, the neutral Au atom in a $5d^96s^2\,^2D_{5/2}$ state has a B of −1049.781(11) MHz.[67] In other words, one d^{-1} hole gives a GHz. Many of the red dots in Figure 5 are far smaller than that.

Concerning the spin−orbit effects and other relativistic effects on q, at the level of multiplicative correction factors, we refer to Pyykkö and Seth.[68]

The MNC ← MCN conversion has been calculated by Jana et al.[69] Hill et al.[70] quote a B_e of 2.80 MHz for an unspecified nucleus. They discuss the vibrational dynamics in detail.

https://doi.org/10.1021/acs.inorgchem.3c02889
Inorg. Chem. 2023, 62, 21083−21090

Wang[46] observed photoelectron spectra in $[Au(CN)_2]^-(g)$ and found in calculations significant covalent character in the Au−C bond.

3.4. Recent Further Examples on δ^4 Rings. Kalita et al.[82] suggest RhSc as a sextuply bonded diatomic with a Rh → Sc δ HOMO. Likewise, Tzeli and Karapetsas[20] find $X^1\Sigma^+$ ground states for RuC, RhB, and PdBe, all three having nonbonding δ^4 HOMOs. For systems of the [MUM] type with M = Rh, Ir, see Shen et al.[83] and references there.

4. CONCLUSIONS

The δ^4 ring lies energetically and radially in the valence range of the 5d elements discussed despite being formally a filled core orbital.[81] Yet it yields mostly no covalent bonding contributions, although the Coulomb attraction to the neighbors must be substantial. In its way, this δ^4 ring resembles the σ^2 lone pairs. An open question is, what kind of chemistry could one do with the δ^4?

AUTHOR INFORMATION

Corresponding Authors

Michiko Atsumi − *Hylleraas Centre for Quantum Molecular Sciences, Department of Chemistry, University of Oslo, Oslo 0315, Norway;* orcid.org/0000-0003-3237-7278; Email: michiko.atsumi@kjemi.uio.no

Pekka Pyykkö − *Department of Chemistry, Faculty of Science, University of Helsinki, Helsinki 00014, Finland;* orcid.org/0000-0003-1395-8712; Email: pekka.pyykko@helsinki.fi

Complete contact information is available at: https://pubs.acs.org/10.1021/acs.inorgchem.3c02889

Author Contributions

M.A. performed the quantum chemical calculations and P.P. provided the conceptualization and background. Both authors contributed to the writing.

Notes

The authors declare no competing financial interest.

ACKNOWLEDGMENTS

The work in Oslo was supported by the Research Council of Norway through its Centers of Excellence scheme, project number 262695. The computations were performed on resources provided by Sigma2—the National Infrastructure for High Performance Computing and Data Storage in Norway through a grant of computer time (grant no. NN4654K). PP is Professor Emeritus at the University of Helsinki. We thank Dr. Erik van Lenthe for advice on ADF, and Prof. Toshiaki Okabayashi for valuable correspondence.

ADDITIONAL NOTES

[a]The PW in the sequel refers to "present work" at this PBE0/TZ2P level.

[b]For brevity, we use here the atomic spectroscopy notation NQCC = $e^2qQ/h = B$.

REFERENCES

(1) Pyykkö, P.; Riedel, S.; Patzschke, M. Triple-bond covalent radii. *Chem. Eur J.* **2005**, *11*, 3511−3520.

(2) Pyykkö, P. Additive covalent radii for single-double-and triple-bonded molecules and tetrahedrally bonded crystals: A summary. *J. Phys. Chem. A* **2015**, *119*, 2326−2337.

(3) Pyykkö, P. Ab initio study of bonding trends among the 14-electron diatomic systems: from B_2^{4-} to F_2^{4+}. *Mol. Phys.* **1989**, *67*, 871−878.

(4) Pauling, L. *The Nature of the Chemical Bond*; 3rd Ed.; Cornell Univ. Press: Ithaca, NY, 1960.

(5) Long, L. H.; Walsh, A. D. Remarks on the structure of carbon monoxide. *Trans. Faraday Soc.* **1947**, *43*, 342−351.

(6) Cotton, F. A.; Murillo, C. A.; Walton, R. A. *Multiple Bonds between Metal Atoms*; 3rd Ed.; Springer: New York, 2005; p 818. See Ch. 8 by R.A. Walton for Re compounds.

(7) Schwerdtfeger, P.; Pernpointner, M.; Nazarewicz, W. Calculation of nuclear quadrupole coupling constants; *Calculation of NMR and EPR Parameters. Theory and Applications*; Wiley, Weinheim, 2004; pp 279−291.

(8) Barysz, M.; Pyykkö, P. Strong chemical bonds to gold. High level correlated relativistic results for diatomic $AuBe^+$, AuC^+, $AuMg^+$, and $AuSi^+$. *Chem. Phys. Lett.* **1998**, *285*, 398−403.

(9) Pyykkö, P.; Tamm, T. Can triple bonds exist between gold and main-group elements? *Theor. Chem. Acc.* **1998**, *99*, 113−115.

(10) Ram, R. S.; Liévin, J.; Bernath, P. F. Emission spectroscopy and ab initio calculations on IrN. *J. Mol. Spectrosc.* **1999**, *197*, 133−146.

(11) Barysz, M.; Pyykkö, P. Strong chemical bonds in heavy diatomics: PtSi, PtTh and $AuTh^+$. *Chem. Phys. Lett.* **2003**, *368*, 538−541.

(12) Patzschke, M.; Pyykkö, P. Darmstadtium carbonyl and carbide resemble platinum carbonyl and carbide. *Chem. Commun.* **2004**, 1982−1983.

(13) Schoendorff, G.; Morris, A. R.; Hu, E. D.; Wilson, A. K. A computational study on the ground and excited states of nickel silicide. *J. Phys. Chem. A* **2015**, *119*, 9630−9635.

(14) Bowmaker, G. A.; Boyd, P. D. W.; Sorrenson, R. J. An SCF−MS−Xα study of the bonding and nuclear quadrupole coupling in dihalogenocuprates(I), CuX_2^-(X = Cl, Br), dihalogenoaurates(I), AuX_2^-(X = Cl, Br, I), and bis(cyano)aurate(I), $Au(CN)_2^-$. *J. Chem. Soc., Faraday Trans. 2* **1985**, *81*, 1627−1641.

(15) te Velde, G.; Bickelhaupt, F. M.; Baerends, E. J.; Fonseca Guerra, C.; van Gisbergen, S. J. A.; Snijders, J. G.; Ziegler, T. Chemistry with ADF. *J. Comput. Chem.* **2001**, *22*, 931−967.

(16) Cheung, L. F.; Chen, T.-T.; Kocheril, G. S.; Chen, W.-J.; Czekner, J.; Wang, L.-S. Observation of four-fold boron-metal bonds in $RhB(BO^-)$ and RhB. *J. Phys. Chem. Lett.* **2020**, *11*, 659−663.

(17) Cheung, L. F.; Kocheril, G. S.; Czekner, J.; Wang, L.-S. The nature of the chemical bonding in 5d transition-metal diatomic borides MB (M = Ir, Pt, Au). *J. Chem. Phys.* **2020**, *152*, 174301.

(18) Brugh, D. J.; Morse, M. D. Resonant two-photon ionization spectroscopy of NiC. *J. Chem. Phys.* **2002**, *117*, 10703−10714.

(19) Wang, F.; Steimle, T. C.; Adam, A. G.; Cheng, L.; Stanton, J. F. The pure rotational spectrum of ruthenium monocarbide, RuC, and relativistic ab initio predictions. *J. Chem. Phys.* **2013**, *139*, 174318.

(20) Tzeli, D.; Karapetsas, I. Quadruple bonding in the ground and low-lying excited states of the diatomic molecules TcN, RuC, RhB, and PdBe. *J. Phys. Chem. A* **2020**, *124*, 6667−6681.

(21) Appelblad, O.; Nilsson, C.; Scullman, R. Vibrational and rotational analysis of some band systems of the molecule PtC. *Phys. Scr.* **1973**, *7*, 65−71.

(22) Lindholm, N. F.; Brugh, D. J.; Rothschopf, G. K.; Sickafoose, S. M.; Morse, M. D. Optical spectroscopy of jet-cooled NiSi. *J. Chem. Phys.* **2003**, *118*, 2190−2196.

(23) Pang, H. F.; Liu, A.-W.; Xia, Y.; Cheung, A. S.-C. Laser induced fluorescence spectroscopy of iridium monophosphide. *Chem. Phys. Lett.* **2010**, *494*, 155−159.

(24) Cooke, S. A.; Michaud, J. M.; Gerry, M. C. L. Microwave spectra, nuclear field shift effects, geometries and hyperfine constants of bismuth mononitride, BiN, and bismuth monophosphide, BiP. *J. Mol. Struct.* **2004**, *695−696*, 13−22.

(25) Merriles, D. M.; Nielson, C.; Tieu, E.; Morse, M. D. Chemical bonding and electronic structure of the early transition metal borides: ScB, TiB, VB, YB, ZrB, NbB, LaB, HfB, TaB, and WB. *J. Phys. Chem. A* **2021**, *125*, 4420−4434.

(26) Liu, R.-Q.; Qin, L.; Zhang, Z.-Y.; Zhao, L.-L.; Sagan, F.; Mitoraj, M.; Frenking, G. Genuine quadruple bonds between two main-group atoms. Chemical bonding in AeF^- (Ae = Be - Ba) and isoelectronic EF (E = B - Tl) and the particular role of d orbitals in covalent interactions of heavier alkaline-earth atoms. *Chem. Sci.* **2023**, *14*, 4872−4887.
(27) Ruipérez, F.; Merino, G.; Ugalde, J. M.; Infante, I. Molecules with high bond orders and ultrashort bond lengths: CrU, MoU, and WU. *Inorg. Chem.* **2013**, *52*, 2838−2843.
(28) Sundholm, D.; Pyykkö, P.; Laaksonen, L. Fully numerical HFS calculations on Cr_2: Basis-set truncation error on the bond length and interaction of the semicore orbitals. *Finn. Chem. Lett.* **1985**, *1985*, 51−55.
(29) Gingerich, K. A. Mass spectrometric evidence for the very high stability of gaseous ThIr and ThPt and method of calculating dissociation energies of diatomic intermetallic compounds with multiple bonds. *Chem. Phys. Lett.* **1973**, *23*, 270−274.
(30) Pyykkö, P.; Patzschke, M.; Suurpere, J. Calculated structures of $[Au = C=Au]^{2+}$ and related systems. *Chem. Phys. Lett.* **2003**, *381*, 45−52.
(31) Pyykkoe, P.; Li, J.; Runeberg, N. Quasirelativistic pseudopotential study of species isoelectronic to uranyl and the equatorial coordination of uranyl. *J. Phys. Chem.* **1994**, *98*, 4809−4813.
(32) Gagliardi, L.; Pyykkö, P. Theoretical search for very short metal-actinide bonds: NUIr and isoelectronic systems. *Angew. Chem., Int. Ed.* **2004**, *43*, 1573−1576 German ed.: Angew. Chem, 116, 1599−1602.
(33) Heinemann, C.; Schwarz, H. NUO^+, a new species isoelectronic to the uranyl dication. UO_2^{2+}. *Chem. Eur J.* **1995**, *1*, 7−11.
(34) Zhou, M.-F.; Andrews, L. Infrared spectra and pseudopotential calculations for NUO^+, NUO, and NThO in solid neon. *J. Chem. Phys.* **1999**, *111*, 11044−11049.
(35) Santos, M.; Marçalo, J.; Pires de Matos, A.; Gibson, J. K.; Haire, R. G. Actinide-transition metal heteronuclear ions and their oxides $[IrUO]^+$ as an analogue to uranyl. *Eur. J. Inorg. Chem.* **2006**, *2006*, 3346−3349.
(36) Wei, F.; Wu, G.-S.; Schwarz, W. H. E.; Li, J. Geometries, electronic structures, and excited states of UN_2, NUO^+, and UO_2^{2+}: a combined CCSD(T), RAS/CASPT2 and TDDFT study. *Theor. Chem. Acc.* **2011**, *129*, 467−481.
(37) Maria, L.; Marçalo, J. Uranyl analogue complexes - Current progress and synthetic challenges. *Inorganics* **2022**, *10*, 121.
(38) Motta, L. C.; Autschbach, J. Actinide inverse trans influence versus cooperative pushing from below and multi-center bonding. *Nat. Commun.* **2023**, *14*, 4307.
(39) Hrobárik, P.; Straka, M.; Pyykkö, P. Computational study of bonding trends in the metalloactinyl series EThM and MThM' (E = N^-, O, F^+; M, M' = Ir^-, Pt, Au^+). *Chem. Phys. Lett.* **2006**, *431*, 6−12.
(40) Surucu, G.; Gencer, A.; Surucu, O.; Ali, M. A. DFT insights into noble gold-based compound Li_5AuP_2: Effect of pressure on physical properties. *ACS Omega* **2023**, *8*, 15673−15683.
(41) Pauling, L. Valence-bond theory of compounds of transition metals. *Proc. Natl. Acad. Sci. U.S.A.* **1975**, *72*, 4200−4202.
(42) Greenwood, N. N.; Earnshaw, A. *Chemistry of the Elements*; Butterworth Heinemann: Oxford, 1997; See pp. 599, Vol. *1266*, p 1274.
(43) Xiong, X.-G.; Wang, Y.-L.; Xu, C.-Q.; Qiu, Y.-H.; Wang, L.-S.; Li, J. On the gold-ligand covalency in linear $[AuX_2]^-$ complexes. *Dalton Trans.* **2015**, *44*, 5535−5546.
(44) Schröder, D.; Brown, R.; Schwerdtfeger, P.; Wang, X.-B.; Yang, X.; Wang, L.-S.; Schwarz, H. Gold dichloride and gold dibromide with gold atoms in three different oxidation states. *Angew. Chem., Int. Ed.* **2003**, *42*, 311−314 version in German Angew. Chem.
(45) Okabayashi, T.; Okabayashi, E. Y.; Koto, F.; Ishida, T.; Tanimoto, M. Detection of free monomeric silver(I) and gold(I) cyanides, AgCN and AuCN: Microwave spectra and molecular structure. *J. Am. Chem. Soc.* **2009**, *131*, 11712−11718.
(46) Wang, X.-B.; Wang, Y.-L.; Yang, J.; Xing, X.-P.; Li, J.; Wang, L.-S. Evidence of significant covalent bonding in $Au(CN)_2^-$. *J. Am. Chem. Soc.* **2009**, *131*, 16368−16370.
(47) Xiong, X.-G.; Liu, H.-T. Anion photoelectron spectroscopy and theoretical study of HAuCN and $[HAuCN]^-$: Spin-orbit coupling and low-lying excited states. *J. Phys. Chem. A* **2020**, *124*, 4712−4719.
(48) Pang, X.-X.; Guo, M.-G.; Wang, Z.-F.; Wang, F. Low-lying states of MX_2 (M = Ag, Au; X = Cl, Br and I) with coupled-cluster approaches: effect of the basis set, high level correlation and spin−orbit coupling. *Phys. Chem. Chem. Phys.* **2020**, *22*, 26178−26188.
(49) Evans, C. J.; Gerry, M. C. L. Pure rotational spectrum and structure of platinum monocarbonyl, PtCO. *J. Phys. Chem. A* **2001**, *105*, 9659−9663.
(50) Feng, R.-L.; Glendening, E. D.; Peterson, K. A. Coupled cluster studies of platinum-actinide interactions. Thermochemistry of $PtAnO^{n+}$ (*n* = 0−2 and An = U, Np, Pu). *J. Phys. Chem. A* **2021**, *125*, 5335−5345.
(51) Assefa, Z.; Kalachnikova, K.; Haire, R. G.; Sykora, R. E. Hydrothermal synthesis, structural, Raman, and luminescence studies of $Am[M(CN)_2]_3 \cdot 3H_2O$ and $Nd[M(CN)_2]_3 \cdot 3H_2O$ (M = Ag, Au): Bimetallic coordination polymers containing both trans-plutonium and transition metal elements. *J. Solid State Chem.* **2007**, *180*, 3121−3129.
(52) Wang, Z.-L.; Hu, H.-S.; von Szentpály, L.; Stoll, H.; Fritzsche, S.; Pyykkö, P.; Schwarz, W. H. E.; Li, J. Understanding the uniqueness of 2p elements in Periodic Tables. *Chem.—Eur. J.* **2020**, *26*, 15558−15564.
(53) Pyykko, P. Relativistic effects in structural chemistry. *Chem. Rev.* **1988**, *88*, 563−594 See Table 4.
(54) Stüker, T.; Beckers, H.; Riedel, S. A cornucopia of iridium nitrogen compounds produced from laser-ablated iridium atoms and dinitrogen. *Chem.—Eur. J.* **2020**, *26*, 7384−7394.
(55) Huber, K. P.; Herzberg, G. *Molecular Spectra and Molecular Structure. IV. Constants of Diatomic Molecules*; Van Nostrand Reinhold: New York, 1979; p 716.
(56) Zaleski-Ejgierd, P.; Patzschke, M.; Pyykkö, P. Structure and bonding of the *M*CN molecules, *M*=Cu, Ag, Au, Rg. *J. Chem. Phys.* **2008**, *128*, 224303.
(57) Schwerdtfeger, P.; Boyd, P. D. W.; Burrell, A. K.; Robinson, W. T.; Taylor, M. J. Relativistic effects in gold chemistry. 3. Gold(I) complexes. *Inorg. Chem.* **1990**, *29*, 3593−3607.
(58) Merriles, D. M.; Morse, M. D. CrN, CuB, and AuB: A tale of two dissociation limits. *J. Phys. Chem. Lett.* **2023**, *14*, 7361−7367.
(59) Gusmão, E. F.; Santiago, R. T.; Haiduke, R. L. A. Accurate nuclear quadrupole moment of ruthenium from the molecular method. *J. Chem. Phys.* **2019**, *151*, 194306.
(60) Schwerdtfeger, P.; Pernpointner, M.; Laerdahl, J. K. The accuracy of current density functionals for the calculation of electric field gradients: A comparison with ab initio methods for HCl and CuCl. *J. Chem. Phys.* **1999**, *111*, 3357−3364.
(61) Haas, H.; Sauer, S. P. A.; Hemmingsen, L.; Kellö, V.; Zhao, P. W. Quadrupole moments of Cd and Zn nuclei: When solid-state, molecular, atomic, and nuclear theory meet. *Europhys. Lett.* **2017**, *117*, 62001.
(62) O'Shea, C. A.; Fromsejer, R.; Sauer, S. P. A.; Mikkelsen, K. V.; Hemmingsen, L. Calculation of electric field gradients in Cd(II) model complexes of the CueR protein metal site. *Phys. Chem. Chem. Phys.* **2023**, *25*, 12277−12283.
(63) Wang, X.-F.; Andrews, L. Gold is noble but gold hydride anions are stable. *Angew. Chem., Int. Ed.* **2003**, *42*, 5201−5206.
(64) Liu, H.-T.; Wang, Y.-L.; Xiong, X.-G.; Dau, P. D.; Piazza, Z. A.; Huang, D.-L.; Xu, C.-Q.; Li, J.; Wang, L.-S. The electronic structure and chemical bonding in gold dihydride: AuH_2^- and AuH_2. *Chem. Sci.* **2012**, *3*, 3286−3295.
(65) Okabayashi, T.; Nakane, A.; Kubota, H.; Mitani, Y.; Yamamoto, T.; Matsumoto, S.; Tanimoto, M. Fourier transform microwave spectroscopy of AgCN and AuCN. *J. Mol. Struct.* **2018**, *1164*, 539−545.
(66) Sunaga, A.; Salman, M.; Saue, T. 4-component relativistic Hamiltonian with effective QED potentials for molecular calculations. *J. Chem. Phys.* **2022**, *157*, 164101.
(67) Childs, W. J.; Goodman, L. S. Hyperfine structure of the 9161 cm^{-1} $^2D_{5/2}$ state of Au^{197} and the nuclear electric-quadrupole moment. *Phys. Rev.* **1966**, *141*, 176−180.

https://doi.org/10.1021/acs.inorgchem.3c02889
Inorg. Chem. 2023, 62, 21083−21090

(68) Pyykkö, P.; Seth, M. Relativistic effects in nuclear quadrupole coupling. *Theor. Chem. Acc.* **1997**, *96*, 92−104.
(69) Jana, G.; Pan, S.; Osorio, E.; Zhao, L.-L.; Merino, G.; Chattaraj, P. K. Cyanide-isocyanide isomerization: stability and bonding in noble gas inserted metal cyanides (metal = Cu, Ag, Au). *Phys. Chem. Chem. Phys.* **2018**, *20*, 18491−18502.
(70) Grant Hill, J.; Mitrushchenkov, A. O.; Peterson, K. A. Ab initio ro-vibrational spectroscopy of the group 11 cyanides: CuCN, AgCN, and AuCN. *J. Chem. Phys.* **2013**, *138*, 134314.
(71) Adam, A. G.; Downie, L. E.; Granger, A. D.; Grein, F.; Slaney, M. E.; Linton, C.; Tokaryk, D. W. A high resolution visible spectrum of iridium monophosphide. *J. Mol. Spectrosc.* **2010**, *263*, 111−119.
(72) Okabayashi, T.; Yamamoto, T.; Okabayashi, E. Y.; Tanimoto, M. Low-energy vibrations of the Group 10 metal monocarbonyl MCO (M = Ni, Pd, and Pt): Rotational spectroscopy and force field analysis. *J. Phys. Chem. A* **2011**, *115*, 1869−1877.
(73) Evans, C. J.; Gerry, M. C. L. Confirmation of the existence of gold (I) fluoride, AuF: microwave spectrum and structure. *J. Am. Chem. Soc.* **2000**, *122*, 1560−1561.
(74) Evans, C. J.; Gerry, M. C. L. The pure rotational spectra of AuCl and AuBr. *J. Mol. Spectrosc.* **2000**, *203*, 105−117.
(75) Reynard, L. M.; Evans, C. J.; Gerry, M. C. L. The pure rotational spectrum of AuI. *J. Mol. Spectrosc.* **2001**, *205*, 344−346.
(76) Parish, R. V. Gold and Mössbauer spectroscopy. *Gold Bull.* **1982**, *15* (2), 51−63.
(77) Bowmaker, G. A.; Whiting, R. Bonding in d^{10} transition metal complexes. IV. Infrared, Raman and N.Q.R. studies of some dihaloaurate(I) complexes. *Aust. J. Chem.* **1976**, *29*, 1407−1412.
(78) Pyykkö, P. Year-2017 nuclear quadrupole moments. *Mol. Phys.* **2018**, *116*, 1328−1338.
(79) Puchalski, M.; Komasa, J.; Pachucki, K. Hyperfine structure of the first rotational level in H_2, D_2 and HD molecules and the deuteron quadrupole moment. *Phys. Rev. Lett.* **2020**, *125*, 253001.
(80) Dognon, J.-P.; Pyykkö, P. Determining nuclear quadrupole moments of Bi and Sb from molecular data. *Phys. Chem. Chem. Phys.* **2023**, *25*, 2758−2761.
(81) Jones, P. G.; Maddock, A. G.; Mays, M. J.; Muir, M. M.; Williams, A. F. Structure and bonding in gold(I) compounds. Part 2. Mössbauer spectrum of linear gold(I) complexes. *Dalton Trans.* **1977**, *1977*, 1434−1439.
(82) Kalita, A.; Gohain, N.; Bordoloi, A.; Bania, K. K.; Guha, A. K. Hetero-polar sextuple bond: A relativistic quantum chemical study. *ChemPhysChem* **2023**, *24*, No. e202200873.
(83) Shen, J.-H.; Rajeshkumar, T.; Feng, G.-F.; Zhao, Y.; Wang, S.-A.; Maron, L.; Zhu, C.-Q. Complexes featuring a *cis*-[M = U=M] core (M = Rh,Ir): A new route to uranium-metal multiple bonds. *Angew. Chem., Int. Ed.* **2023**, *62*, No. e202303379.

Recommended by ACS

Electronic Structure of Actinyls: Orbital Properties
Paul S. Bagus, Tonya Vitova, *et al.*
JANUARY 17, 2024
INORGANIC CHEMISTRY
READ

Structures and Energetics of $E_2H_3^+$ (E = As, Sb, and Bi) Cations
Shu-Hua Xia, Henry F. Schaefer III, *et al.*
JANUARY 16, 2024
THE JOURNAL OF PHYSICAL CHEMISTRY A
READ

Three-Center M–H–B Bonds Are Strong Field Interactions. Synthesis and Characterization of $M(CH_2NMe_2BH_3)_3$ Complexes of Titanium, Chromium, and Cobalt
R. Joseph Lastowski, Gregory S. Girolami, *et al.*
OCTOBER 18, 2023
JOURNAL OF THE AMERICAN CHEMICAL SOCIETY
READ

Heteronuclear and Homonuclear Bimetallic Metallocenes of Alkaline Earths and Zinc
Matthew A. Gosch and David J. D. Wilson
AUGUST 17, 2023
ORGANOMETALLICS
READ

Get More Suggestions >

https://doi.org/10.1021/acs.inorgchem.3c02889
Inorg. Chem. 2023, 62, 21083−21090